ELSEVIER

International Journal of Mass Spectrometry 205 (2001) 65–75

International Journal of Mass Spectrometry

Dissociative electron attachment to N_2O clusters: attachment spectra for $(N_2O)_nO^-$ anions ($n = 0$–7) from about 0 up to 25 eV

G. Hanel, T. Fiegele, A. Stamatovic[1], T.D. Märk*,[2]

Institut für Ionenphysik, Universität Innsbruck, Technikerstrasse 25, A-6020 Innsbruck, Austria

Received 17 March 2000; accepted 12 May 2000

Abstract

Using a recently constructed high resolution crossed beams apparatus involving a hemispherical electron monochromator we have studied from threshold up to 25 eV electron attachment to N_2O clusters in the size range up to about 10. Attachment spectra obtained for the production of $(N_2O)_nO^-$ exhibit with increasing cluster size a gradual redshift of the maximum peak position of the major rather broad resonance located at around 2 eV, i.e. values varying from 2.58 ± 0.1 eV for O^- to 1.70 ± 0.1 eV for $(N_2O)_7O^-$. In addition, with increasing cluster size the anion signal is more fully developed near 0 eV, i.e., whereas for $n = 0$ the O^- ion signal is zero at about zero energy (in accordance with expectations from thermochemical data), there exists an appreciable ion signal at zero energy for $n = 7$. Above the 2 eV resonance there exists a shallow minimum in the cross section at about 4 eV with a slightly increasing, probably structured, broad feature toward higher energies. The present results are compared to previous attachment studies concerning the monomer and clusters of N_2O and to O^- desorption studies from condensed N_2O thereby elucidating the origin and evolution (under different phase conditions) of the various features of the attachment spectra. (Int J Mass Spectrom 205 (2001) 65–75) © 2001 Elsevier Science B.V.

Keywords: Electron attachment; N_2O clusters; Electron monochromator; Cross sections

1. Introduction

Electron impact ionization and electron attachment is an important tool in the study of molecules and clusters, in particular concerning the production and identification of the corresponding cations and anions in mass spectrometry and related studies about the properties of these ions (determination of cross sections, fragmentation patterns, structure, reactivity, energetics, etc.) [1–6]. Details of the electronic and vibrational structures of cations have, however, usually been deduced using photoionization due to the much better energy resolution available. This is particularly true for the determination of appearance energies (AE) and related data on the energetics of positive ions (see discussion in [7]). Nevertheless, as discussed in detail in [8,9], with the recent progress concerning high resolution electron guns (achieving for instance with a hemispherical monochromator

* Corresponding author.

[1] Permanent address: Faculty of Physics Beograd, P.O. Box 368, 11001 Beograd, Yugoslavia.

[2] Also adjunct professor at Dept. Plasma Physics, Comenius University, Mlynska dolina, SK-84215 Bratislava, Slovakia.

Dedicated to Professor Aleksandar Stamatovic on the occasion of his 60th birthday.

PII S1387-3806(00)00274-8

well monochromatized electron beams with appreciable currents allowing to also study reactions with small cross sections) it is now also possible to perform high resolution measurements with free electron beams on rather elusive species such as atomic or molecular clusters. Particular successful examples for investigations along this line are recent electron attachment studies in our laboratory using a trochoidal electron monochromator where we were able to measure vibrationally resolved electron/cluster attachment spectra for oxygen [10,11] and nitric oxide clusters [12,13] thus allowing quantitative information to be obtained about the underlying attachment reactions (attachment mechanisms, energetics, cross sections).

Here we apply this new generation of crossed electron/molecular beam type machines involving the hemispherical monochromator [8,9] to the investigation of the electron attachment (measurement of attachment spectra) to $(N_2O)_n$ clusters in the size range up to $n = 8$ and an electron energy range up to about 25 eV with an energy resolution of about 100–150 meV. Whereas numerous studies exist on the electron attachment to the N_2O monomer (see for instance the recent paper [14] and references given therein) and on the electron impact ionization of gaseous N_2O (see for instance all the appearance measurements listed in [15]), the number of previous studies concerning the attachment of free electrons to N_2O clusters is limited. Besides a pioneering study of Klots and Compton [16] using the retarding potential difference (RPD) technique, there exists a study by Knapp et al. [17–19] and a recent ultrahigh resolution laser photoelectron study by Hotop and co-workers [20]. In addition two investigations involving bound electron transfer in Rydberg electron transfer studies to N_2O clusters have been reported in the literature [21–23].

The present study with a recently constructed hemispherical electron analyzer [8,9,24–26] constitutes on the one hand a systematic extension of the previous measurements in terms of range of energy (i.e. the measurements of [20] are limited to an energy range of only up to 180 meV and the ones of [16] and [17–19] to about 2.5 and 5 eV, respectively), in terms of resolution (e.g. the measurements of [17–19] have been carried out with an ordinary electron gun with a full width at half maximum (FWHM) of the electron energy distribution of ~1 eV) and in terms of cluster size (e.g. in [16] only two cluster ions are reported). On the other hand the present study has been initiated in order to clarify a more general question involving negative ion formation from low energy electron impact to molecules under different phase conditions. Desorption of O^- from condensed N_2O [27,28] predominantly occurs in the energy range between 6 and 12 eV, whereas gas phase dissociative electron attachment (DEA) has its major contribution at energies of around 2 eV [14] with some minor contributions in the higher energy range (according to [29] there are peaks at 5.4, 8.1, and 13 eV having peak values which are about three orders of magnitude smaller than the peak value at around 2 eV). Similar phenomena were recently observed for halogenated methanes [30–32] and attributed to core excited resonances. In the gas phase these resonances are short lived and decay by autodetachment into the associated electronically excited state of the neutral yielding low energy electrons. Under aggregation, these states may no longer decay via such a one electron transition (i.e. the open channel situation has been changed by polarization forces to a closed channel type situation) thereby significantly enhancing the autodetachment lifetime and thus the probability for DEA. Recently, this question has been addressed in the case of electron attachment to CF_2Cl_2 [33] and it has been shown that features virtually absent in the gas phase, are seen from clusters and become the dominant process in desorption.

2. Experimental

2.1. Apparatus

The apparatus used for the present experiments, schematically shown in Fig. 1 (see also [8,9,24–26]), consists of an electron gun, a collision chamber, and an electron collection system. This system was primarily built in our Innsbruck laboratory for the study of electron–cluster interactions under high sensitivity

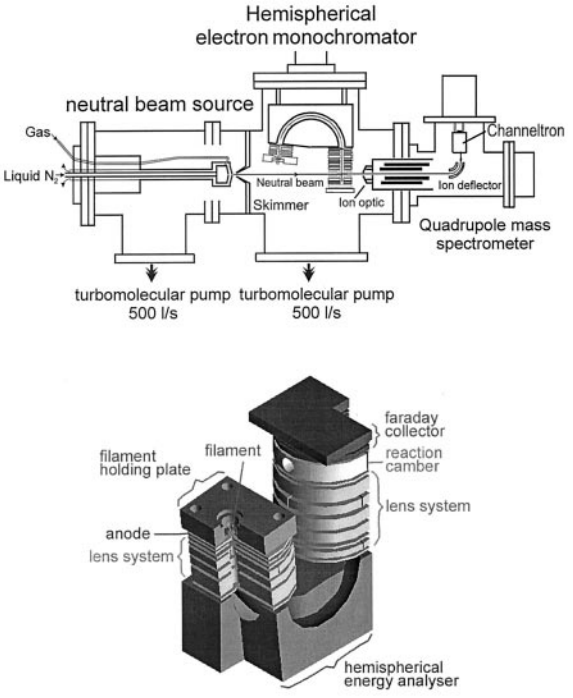

Fig. 1. Schematic diagram of the instrument. Electrons are emitted from a hot filament, and focused into a beam. They pass the hemispherical energy selector at a constant energy of about 4 eV and are focused and brought to the final collision energy before they interact with the neutral beam and are collected at a Faraday cup. Also shown is a close-up of the monochromator in a three dimensional view.

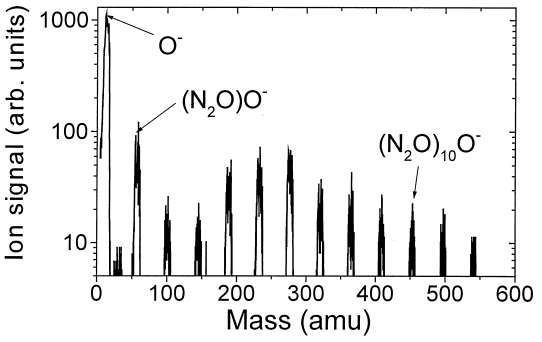

Fig. 2. Mass spectrum for $(N_2O)_nO^-$ cluster anions produced by electron attachment (using 2 eV electrons) to a N_2O cluster beam formed with the stagnation gas temperature at room temperature and the stagnation gas pressure of 3 bar.

and high energy resolution. Clusters are produced in the first of the two differentially pumped chambers by a nonseeded adiabatic expansion of a temperature controlled NO_2 gas through a thin orifice of 20 μm in diameter at a stagnation pressure of about 2–3 bar (see Fig. 2 showing a typical mass spectrum for negative ions). At a distance of 2 cm, the cluster beam is skimmed with a 1 mm diameter skimmer and 8 cm further downstream, shortly before it interacts with the electrons, the beam is collimated to a diameter of 3 mm. The expansion chamber and the interaction region are separately evacuated by 500 l/s turbomolecular pumps.

The monochromatized electrons (with typical currents in the present study of about 50 nA, see the following discussion also) are produced by a standard home-built hemispherical electron monochromator (HEM) whose performance has been improved by careful attention to a number of technical details. The hemispheres, the sample inlet system and all electron–ion-optical elements are made of a single material (stainless steel). Differential pumping (using turbomolecular pumps) between the different parts and frequent bake-outs are invoked to reduce contamination of the surfaces by the sample gas. Residual magnetic fields in the whole instrument are kept below 0.003 G with Helmholtz coils compensating the earth's magnetic field. Ferromagnetic materials were avoided in the vicinity of the electron beam. All voltages applied to the electron-ion-optical elements are supplied by a specially constructed power supply with a ripple of $\leq$1 mV.

Positive or negative ions formed in the collision chamber are extracted by a weak electric field. Usually, a rather low ion extraction voltage of about 50 mV (corresponding to an electric field strength of about 0.12 V/cm) was used in order to minimize disturbing field effects, for more details on the influence of this extraction voltage on the energy resolution and energy scale calibration see [24]. The extracted ions are then focused by a system of electrostatic lenses into the entrance of a quadrupole mass spectrometer with a nominal mass range of 2000 u. The mass selected ions are detected by a channeltron multiplier operated in single ion counting mode.

Table 1
Measured appearance energies for positive ions of some rare gases and molecules compared to standard values derived from photoionisation results (taken from NIST tables [37]) using Xe to calibrate the energy scale.

Target	Present AE value (eV)	NIST value (eV)	Difference (meV)	p value
Xe	12.129 87	12.129 87	0	1.12
Ar	15.749 ± 0.012	15.759 ± 0.001	10	1.30
Kr	13.990 ± 0.015	13.999 ± 0.001	9	1.22
N_2	15.590 ± 0.011	15.581 ± 0.008	9	1.18
O_2	12.073 ± 0.021	12.0697 ± 0.0002	3	1.24
N_2O	12.865 ± 0.009	12.889 ± 0.004	23	1.28

2.2. Energy scale calibration and energy resolution

One way to check the performance of the instrument (e.g. in terms of its electron energy resolution) and to calibrate the electron energy scale is the measurement of the Cl^- production via DEA to CCl_4 at incident energies, *E*, close to 0 eV [24]. The width of the "zero-energy" DEA peak is determined by the convolution of the finite electron beam distribution and the rapidly decreasing *s*-wave cross-section function [34–36] so that the FWHM gives a convenient measure for the energy spread of the electron beam. In the present experiment an improved version of our HEM developed recently gave at best an energy spread of about 30 meV. Nevertheless, for the present set of measurements an energy resolution of ~100–150 meV has been used in order to achieve electron currents large enough (~50 nA) to study ions produced with small cross sections.

The zero-energy Cl^-/CCl_4 peak position was also used for calibration of the energy scale at low energies, whereas the O^- onset for DEA to CO at about 9.6 eV and appearance energies for the production of cations of various test gases (including rare gases and molecular gases, see Table 1 showing results obtained previously in our laboratory [8,9,24] and compared to high accuracy literature data [37]) have been used for calibration of the electron scale at higher energies. Fig. 3 shows the results for the energy dependence of the O^- cross section for DEA to CO. Also shown is the DA signal for Cl^- from CCl_4, indicating an energy resolution of about 80 meV in the low energy region close to 0 eV for this experimental run. The O^-/CO cross-section curve shows, in accordance with the earlier measurements of Stamatovic and Schulz [38], a sharp onset near 9.6 eV. However, the trailing edge of the present O^- resonance does not agree with that reported in [38]. This is probably due to the weak extraction field which we are using in our current work, leading to the loss of ions formed with larger kinetic energy. Similar discrimination effects have been observed and discussed in detail in a previous investigation with this apparatus concerning electron attachment to NO [24].

As can be seen from Fig. 3, the FWHM of the derivative of the apparent "step function" near threshold is, with 118 meV, only slightly larger than the FWHM of the "zero energy peak" of CCl_4 under the same experimental conditions of the monochromator,

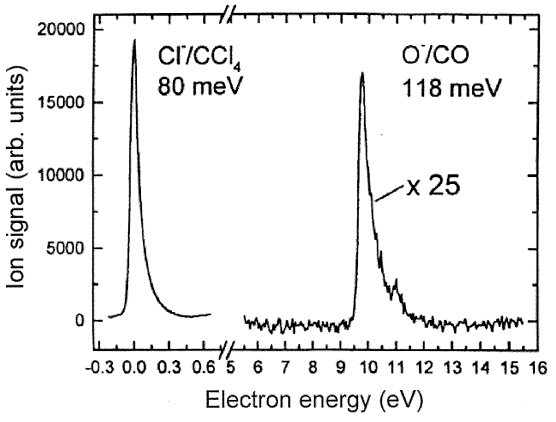

Fig. 3. Formation of O^- from CO by electron impact. The Cl^-/CCl_4 cross-section curve near 0 eV is used to calibrate the electron energy scale and to determine the electron energy resolution (80 meV) at low energy, whereas the onset of the O^-/CO curve at 9.63 eV gives information on the energy resolution (118 meV) in this high energy range.

thus indicating the true vertical character of this onset corresponding to a particular type of transition in the potential energy diagram as discussed in detail in [38]. Chantry [39] has pointed out that for a DEA cross section, which features such a step function near threshold, the true onset corresponds to the steepest part of the observed curve, provided that the energy scale corresponds to the most probable electron energy (the latter is fulfilled due to the energy calibration used here; i.e. not using the maximum of the zero-energy peak cross section of Cl^- from CCl_4 but the steepest part of the leading edge). Deriving the onset in this way we obtain a value of 9.63 eV for the onset of O^-/CO in excellent agreement with the benchmark value of 9.63 eV reported by Stamatovic and Schulz [38] using a trochoidal monochromator with a nominal resolution of 70 meV. These experimental onset values compare very favorably with a value of 9.63 eV derived from the difference between the bond dissociation energy D(C–O) = 11.09 eV [40] and the electron affinity EA(O) = 1.461 eV [41] thus demonstrating the reliability of the experimental technique used and at the same time giving an estimate for the upper limit of the energy scale accuracy of about 10 meV. This upper limit for the accuracy is also in excellent agreement with the accuracy limit estimated from the appearance energy measurements shown in Table 1.

3. Results and discussion

3.1. Mass spectrum

The negative ion mass spectrum shown in Fig. 2 has been taken with an electron energy of 2 eV corresponding approximately to the maximum of the major peak in the electron attachment cross section functions (see the following discussions and Fig. 4). This mass spectrum consists solely of anions of the form $(N_2O)_nO^-$, only for the monomer a small NO^- signal can be seen. Knapp et al. [17–19] using much higher electron currents (at the low energy resolution of about 1 eV FWHM) were able to see also ions of the form $(N_2O)_nNO^-$ and $(N_2O)_n^-$ albeit with abundances of two and three orders of magnitude lower than the dominant anion series $(N_2O)_nO^-$. A similar observation concerning the relative abundance of $(N_2O)_nO^-$ and $(N_2O)_n^-$ anions has been reported by Weber et al. [20] for very sharp peaks at electron energies very close to zero and by Kraft et al. [22,23] for Rydberg electron transfer. In this case Weber et al. associated this fact to the production of nuclear-excited Feshbach resonances of temporary cluster ions $(N_2O)_n^-$ dissociating into $(N_2O)_mO^-$ [20]; see also discussions on the ion production channels in earlier works, in particular by Klots and Compton [16] involving "ion molecule half reactions."

Moreover, in contrast to the positive ion mass spectrum (see e.g. Fig. 2 in [42]) which exhibits a gradually decreasing abundance of the cluster ion with increasing cluster size, in the negative ion mass spectrum a distinct relative minimum can be seen at a cluster size of $n = 3$ and 4 and a relative maximum at $n = 6$ and 7 (see also the same results obtained by Knapp et al. [17]). A similar observation by Weber et al. [20] and Kraft et al. [22,23] for anions produced close to zero electron energy by attachment of either free electrons or Rydberg electrons with high principal quantum numbers, respectively—i.e. they report the following relative anion signals for $(N_2O)_nO^-$ ions with $n = 4$–9: 169, 1000, 907, 133, 117, and 71 and for $(N_2O)_n^-$ ions with $n = 4$–9: 4, 27, 45, 359, 157, and 79—has been interpreted in such a way that the vertical electron affinities of $(N_2O)_n$ become positive at the neutral cluster size $n = 7$ thus leading to a size selective enhancement of the attachment process at this cluster size. This, however, will not explain the presently (see Fig. 2) observed strong ion signal for the dimer anion and the much smaller variation in ion signal between the maximum and minimum peak (approximately a factor of 2). Rather, we attribute this variation in abundance partly with associated different stabilities of the nascent anions and note in this conjunction that according to Weber et al. [20] the closing of a first solvation shell is predicted for size $n = 6$. As will be discussed in sec. 3.2, another reason for this variation could be the strong energy dependence of the cross section and its variation with cluster size.

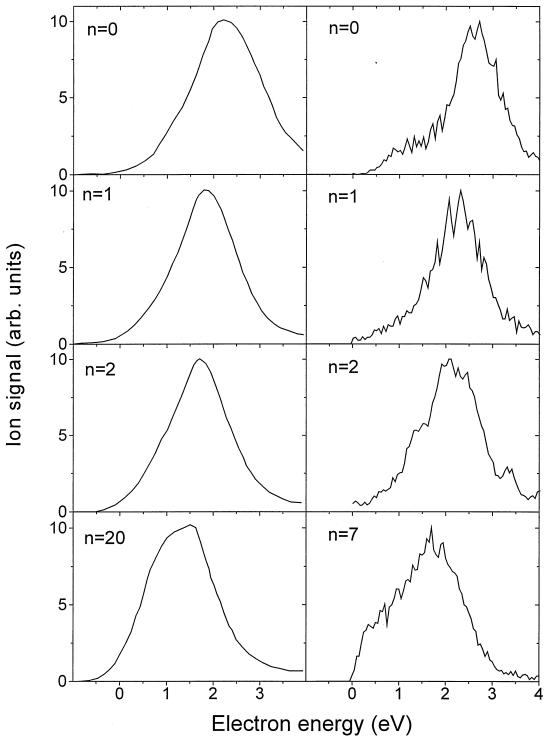

Fig. 4. Energy dependence of the $(N_2O)_nO^-$ yield for various cluster sizes (all curves are normalized to the same maximum value). Left-hand side results by Knapp et al. [18,19] and right hand side present results. Note the different energy calibration used in both studies (see text).

3.2. Electron attachment spectra

Fig. 4 shows as an example some of the measured electron attachment spectra for cluster anions $(N_2O)_nO^-$ with sizes $n = 0$, 1, 2, and 7. The energy scale has been calibrated as mentioned above by using CCl_4 and CO electron attachment spectra. Also shown for comparison are corresponding data reported by Knapp et al. [18,19]. Two observations are noteworthy. Both data sets exhibit with increasing cluster size (1) a gradual redshift (due to solvation effects) of the maximum peak position (see Table 2) and (2) they are more fully developed near 0 eV (that is whereas for $n = 0$ the ion signal is zero at about zero energy, there exists an appreciable ion signal at zero energy for $n = 7$). The former effect will—as can be seen from Fig. 4—lead to the fact that a mass spectrum

Table 2
Energy positions of the peak maxima for the DEA reaction proceeding through the $^2\Sigma$ resonance as a function of cluster size.

Cluster size $(N_2O)_nO^-$	Present results (eV)	Results by Knapp et al. [17–19] (eV)	Results by Klots and Compton [16] (eV)
$n = 0$	2.58	2.21	
1	2.32	1.79	1.8
2	2.11	1.70	
3	1.96		
4	1.81		
5	1.80		
6	1.75		
7	1.70		
16			1.2
20		1.50	

(Fig. 2) measured at 2 eV electron attachment energy will give a wrong impression about the relative production efficiencies of the different ions. Only cluster ions with $n = 2$ will be detected in the maximum of their resonance, whereas larger and smaller clusters ions will be detected off-resonance. This effect may also be, in part, responsible for the different size dependence observed in the negative and positive mass spectrum, see the previous discussion.

In the present case the peak energy values vary from 2.58 ± 0.1 eV for O^- to 1.70 ± 0.1 eV for $(N_2O)_7O^-$, in the earlier case [18,19] from 2.25 eV to 1.5 eV for $(N_2O)_{20}O^-$ and ∼1.0 eV for a cluster anion containing a few hundred N_2O molecules. Klots and Compton [16] see a similar behaviour, observing for instance that the $(N_2O)O^-$ signal maximizes at 1.8 eV and the $(N_2O)_{16}O^-$ ion measured without RPD technique at about 1.2 eV. The absolute values for these peak positions are rather different for the three data sets, but the relative shifts are in much better agreement (see Table 2).

One reason for this difference in absolute values is very likely the rather broad energy distribution used in the case of the Knapp et al. [17–19] study, but another more important reason is the different energy scale calibration used in both earlier cases ([16] and [17–19]), i.e. the energy scale for the mean electron energy was set by defining the energy at which O^- maxi-

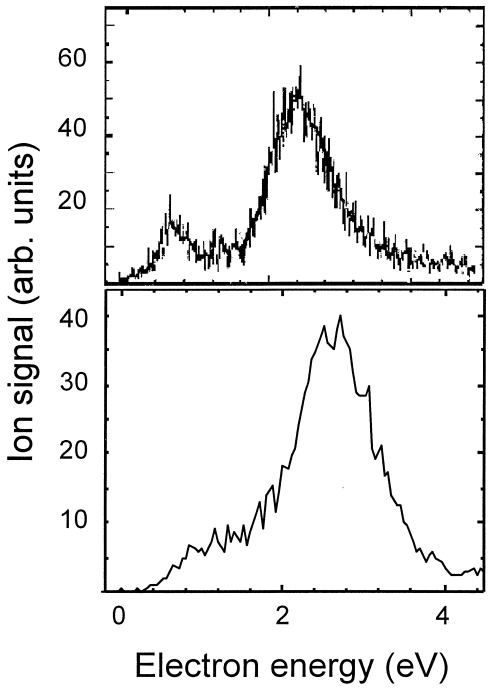

Fig. 5. O^- signal obtained from electron attachment to a stagnant N_2O gas target at ambient gas temperature (upper panel) and from electron attachment to a molecular beam produced by supersonic expansion and thus containing a $(N_2O)_n$ cluster distribution (lower panel). In both cases the energy calibration has been carried out with Cl^- from CCl_4.

mizes to be 2.3 eV. This, however, may lead to an erroneous energy scale as can be seen from Fig. 5, where we compare the production of O^- by electron attachment to stagnant N_2O background gas (introduced into the ion source by a capillary leak inlet) and by electron attachment to the N_2O molecular beam produced by supersonic nozzle expansion and thus containing N_2O clusters. It can be clearly seen that the two attachment spectra are strongly differing, in particular concerning the energy value for the maximum of the high energy peak. Whereas the stagnant gas peak maximizes at about 2.4 eV in accordance with the earlier study by Brüning et al. [14], the O^- peak measured with the supersonic nozzle expansion is shifted to the slightly higher value of 2.58 eV. If this latter peak is set to 2.3 eV—as has been done by Knapp et al. [18,19] and by Klots and Compton [16]—this will introduce an error of 0.28 eV in the absolute energy scale.

In addition to the peak maximizing at around 2.4 eV the present stagnant gas spectrum shows in accordance with earlier studies [14] a second peak, the peak energy values being in the earlier study at around 0.55 ± 0.1 and at 2.4 ± 0.1 eV, respectively. Following the earlier interpretation [14] the two contributions are arising from vertical attachment to the linear configuration of the $^2\Pi$ and $^2\Sigma$ compound states of $(N_2O)^-$, respectively, followed by dissociation into O^-. Similar to the isoelectronic CO_2 molecule, the neutral N_2O molecule is linear while N_2O^- is considered (1) to have its potential energy minimum at a bending angle near 133° and to have the bond lengths considerably expanded as compared to (linear) N_2O in its ground state [43,44]. The vertical electron affinity for the $^2\Sigma$ of N_2O is -2.23 eV and for the $^2\Pi$ state about 1 eV, whereas the adiabatic one is $+0.22$ eV. The lowest point of intersection of the surfaces occurs at a bond angle of 154°, with an energy of 0.7 eV above the value of the ground state N_2O. Taking into account the low bond strength between N_2 and O of 1.72 eV and the electron affinity of O with 1.46 eV [41] the energy threshold for dissociative attachment to yield O^- is at 0.26 eV. As shown in [14] the peak at about 2.4 eV is independent of gas temperature and the energy at the maximum corresponds to an attachment energy close to the vertical EA of the molecule. The low-energy resonance, on the other hand showed a strong temperature dependence in the measured temperature range between 307 and 675 K in two ways, i.e. the energy of the maximum shifts towards lower energies with increasing temperature and a threshold peak (at zero energy) appears increasing with increasing temperature and finally at high temperature merging with the shifting $^2\Pi$ resonance to one single peak at zero energy. This energy and temperature dependence is typically for a DEA with an activation barrier and it was shown [14] that the measured activation energy is close to the dissociation limit 0.26 eV.

Comparison in Fig. 5 of the stagnant gas spectrum with the supersonic expansion spectrum reveals an interesting feature concerning this low energy peak. It can be seen that the O^- peak has decreased and shifted to higher energy peaking quite close or even

above the value of the vertical EA of the $^2\Pi$ state responsible for this resonance. In addition, under these target conditions which correspond to a very low temperature environment due to the supersonic expansion, the low energy tail of this resonance extends only down to about 0.2 eV corresponding to the theoretical threshold in the case of negligible vibrational excitation. A similar disappearance of a zero-energy temperature dependent peak in the case of supersonic expansion conditions has already previously reported for the SF_5^- production via dissociative electron attachment to the SF_6 molecule [45]. In contrast, the $(N_2O)O^-$ ion signal (see Fig. 4) does not show such a cutoff, but extends clearly all the way to zero energy suggesting a finite cross section at zero energy in accordance with the earlier RPD measurement of Klots and Compton [16]. Thus, in this case and also for larger clusters solvation energy will counterbalance the energy need due to the thermodynamic threshold of the monomer. It is interesting to note that this is also in accordance with the observations of Weber et al. [20] who only report the observation (in their low energy experiment below 180 meV) of the extremely sharp nuclear excited Feshbach resonances and of *s*-wave scattering close to zero energy for cluster sizes above $n = 4$.

Fig. 6 shows the present attachment yields for an extended electron energy range up to 25 eV. It can be seen that for all cluster sizes studied above the dominating $^2\Sigma$ resonance (located at around 2.6–1.7 eV depending on cluster size) at an energy of about 4 eV there exists a shallow minimum in the cross section with a slightly increasing, probably structured, broad feature towards higher electron energies. The shape of these cross sections measured for clusters resembles very much the completely unstructured shape measured previously for the gas phase molecule [14]. In contrast, the previous studies on electron stimulated desorption of O^- from condensed N_2O [27,28] exhibited as the main feature at least three strong and clear structures located around 7, 9, and 15 eV. It is interesting to speculate that some of the cluster spectra shown in Fig. 6 appear to exhibit at least for the larger cluster sizes a weak but distinct resonant contribution near 7 eV.

Negative ion formation at higher energy, not present in the cross section of the monomer molecule, has been observed for various clusters which exhibit zero-energy peaks [46–48]. Such features have been attributed [46–48] to autoscavenging reactions in the cluster, i.e. inelastic scattering of the initial fast electron at one cluster site (creating there an electronically excited molecule) followed by a capture of the slowed-down electron at another cluster site via the zero-energy resonance. If resolved these features therefore represent threshold excitation spectra of the molecules present in the cluster. In the present cluster system (see Figs. 4 and 6) we do not have the typical situation of a strong zero energy resonance (as for instance observed for oxygen clusters [10,11]) and in addition the only feature (only barely observable) appears at the position of the structures observed for the condensed N_2O. Nevertheless the data sets exhibit with increasing cluster size a gradual redshift of the maximum peak position and they are more fully developed near 0 eV thus in principle allowing the occurrence of autoscavenging.

Despite this, for the present molecule, the structures between 7 and 16 eV reported for the electron-stimulated desorption by [27,28] and therefore also the weak structure seen here in the cluster case cannot be attributed to an autoscavenging process. This can be concluded from the fact that the low-energy resonances are not observed at all in the desorption spectrum (1) due to insufficient kinetic energy release and (2) due to the fact that it was shown in [28] that the higher energy states located between 7 and 16 eV directly decompose into O^- ions (having a broad kinetic energy distribution when they are ejected from the surface). The appearance of these features in the condensed case can be ascribed to the fact that the autodetachment lifetime for a negative ion resonance formed by the initial capture critically depends on the disposition of the neutral and the ion potential energy surface within the Franck-Condon region. Once the transient anion is formed, autodetachment is a competing channel to DEA and may strongly suppress negative ion formation. If, however, due to polarization forces the anion potential is shifted in the condensed case, autodetachment may be less severe

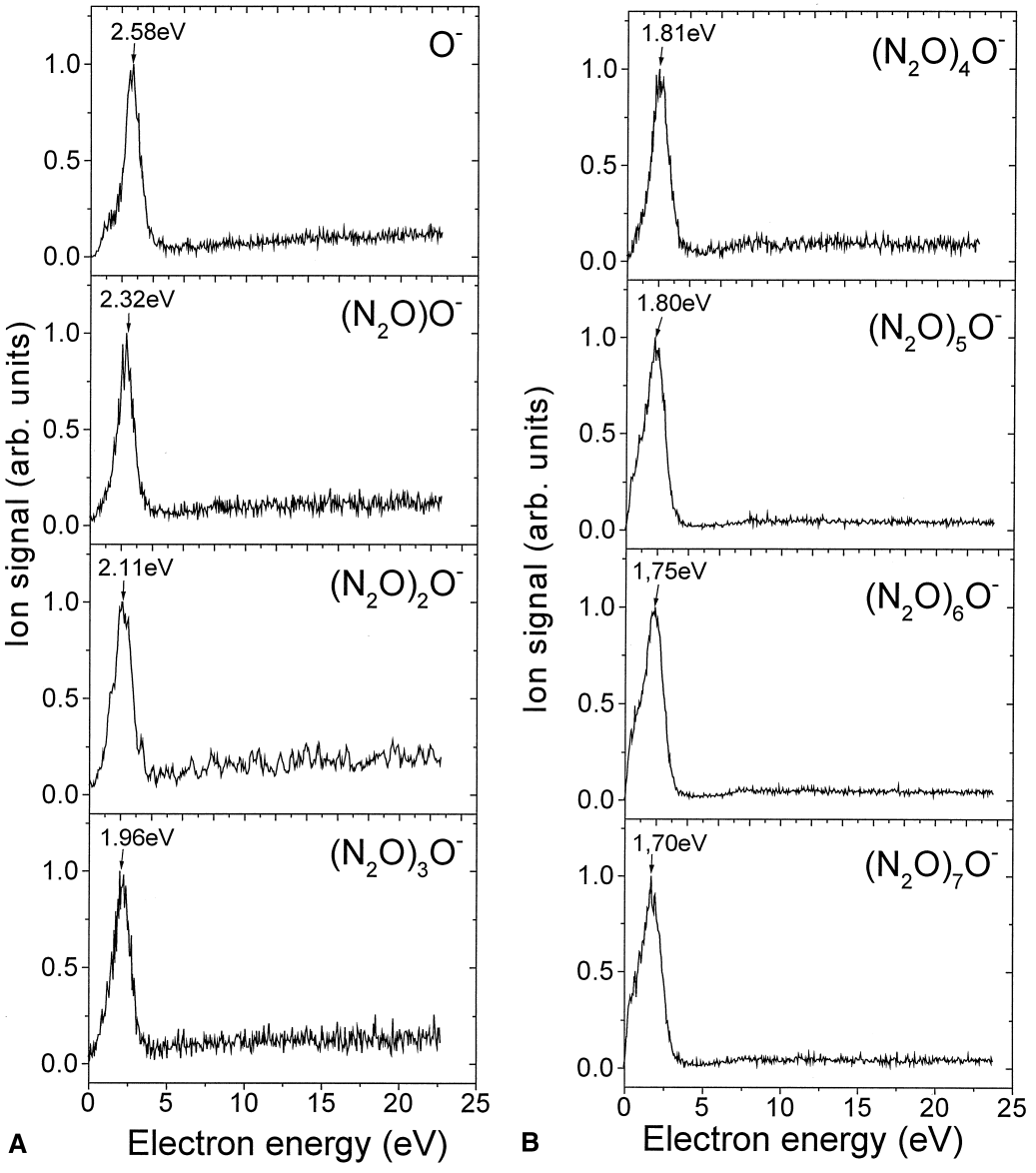

Fig. 6. Energy dependence of the $(N_2O)_nO^-$ yield for various cluster sizes (all curves are normalized to the same maximum value) for an extended range of electron energy (as compared to results shown in Fig. 4 which only cover the range up to 4 eV).

and thus resonances may appear in the desorption spectra. The present observation of a small peak at around 7 eV for larger clusters may be due to the main resonance at 9 eV in the condensed case due to a lesser shift in the potential in the cluster case. Thus we are finally concluding, that the small structure at around 7 eV in the cluster case is due to direct DEA from the same excited states seen in desorption between 7 and 16 eV and that the unstructured general increase above this energy may be due to autoscavenging reactions involving the production of excited states in a neutral molecule (either within the cluster

or in the background gas). The latter interpretation is in line with Chantry [49] who argued that peaks (especially present in those experiments using higher gas pressures and not seen in Ref. [14] where low gas pressure have been used) in the cross section of the N_2O gas phase molecule at higher energies (above 4 eV) may not result from a direct DEA reaction but rather represent peaks due to inelastic energy loss reactions leaving the electron at energies appropriate for the DEA.

Acknowledgements

Work partially supported by the FWF and BMWV, Wien, Austria. It is a pleasure to acknowledge valuable discussions with Dr. Matthias Lezius, Innsbruck, Prof. Dr. Eugen Illenberger, Berlin, and Dr. Nigel Mason, London.

References

[1] Electron Interactions and their Applications, L.G. Christophorou (Ed.), Academic, Orlando, 1984.
[2] T.D. Märk, G.H. Dunn, Electron Impact Ionization, Springer, Wien, 1985.
[3] E. Illenberger, J. Momigny, Gaseous Molecular Ions, Steinkopff, Darmstadt, 1992.
[4] T.D. Märk, Int. J. Mass Spectrom. Ion Processes 79 (1987) 1.
[5] T.D. Märk, in Linking the Gaseous and Condensed Phase of Matter, L.G. Christophorou, E. Illenberger, W.F. Schmidt (Eds.), Plenum, New York, 1994, NATO ASI Series, Vol. 326, p. 155.
[6] Clusters of Atoms and Molecules, H. Haberland (Ed.), Springer, Berlin, 1994.
[7] H.M. Rosenstock, Int. J. Mass Spectrom. Ion Phys. 20 (1976) 139.
[8] D. Muigg, G. Denifl, A. Stamatovic, O. Echt, T.D. Märk, Chem. Phys. 239 (1998) 409.
[9] D. Muigg, G. Denifl, N.J. Mason, A. Stamatovic, T.D. Märk, J. Chem. Phys., submitted.
[10] S. Matejcik, A. Kiendler, P. Stampfli, A. Stamatovic, T.D. Märk, Phys. Rev. Lett. 77 (1996) 3771.
[11] S. Matejcik, P. Stampfli, A. Stamatovic, P. Scheier, T.D. Märk, J. Chem. Phys. 111 (1999) 3548.
[12] Y. Chu, G. Senn, P. Scheier, A. Stamatovic, T.D. Märk, F. Brüning, S. Matejcik, E. Illenberger, Phys. Rev. A 57 (1998) R697.
[13] Y. Chu, G. Senn, S. Matejcik, P. Scheier, P. Stampfli, A. Stamatovic, E. Illenberger, T.D. Märk, Chem. Phys. Lett. 289 (1998) 521.
[14] F. Brüning, S. Matejcik, E. Illenberger, Y. Chu, G. Senn, D. Muigg, G. Denifl, T.D. Märk, Chem. Phys. Lett. 292 (1998) 177.
[15] S.G. Lias, in NIST Chemistry Webbook, NIST Standard Reference Database Number 69, W.G. Mallard, P.G. Linstrom (Eds.), National Institute of Standards and Technology, Gaithersburg, MD, 2000 (http://webbook.nist.gov).
[16] C.E. Klots, R.N. Compton, J. Chem. Phys. 69 (1978) 1636.
[17] M. Knapp, D. Kreisle, O. Echt, K. Sattler, E. Recknagel, Surf. Sci. 156 (1985) 313.
[18] M. Knapp, O. Echt, D. Kreisle, T.D. Märk, E. Recknagel, Chem. Phys. Lett. 126 (1986) 225.
[19] M. Knapp, O. Echt, D. Kreisle, T.D. Märk, E. Recknagel, in Physics and Chemistry of Small Clusters, P. Jena, B.K. Rao, S.N. Khanna (Eds.), Plenum, New York, 1987, p. 693.
[20] J.M. Weber, E. Leber, M.W. Ruf, H. Hotop, Phys. Rev. Lett. 82 (1999) 516.
[21] S. Yamamoto, K. Mitsuke, F. Misaizu, T. Kondow, K. Kuchitsu, J. Phys. Chem. 94 (1990) 8250.
[22] T. Kraft, M.W. Ruf, H. Hotop, Z. Phys. D 17 (1990) 37.
[23] T. Kraft, M.W. Ruf, H. Hotop, Z. Phys. D 20 (1991) 13.
[24] G. Denifl, D. Muigg, A. Stamatovic, T.D. Märk, Chem. Phys. Lett. 288 (1998) 105.
[25] P. Cicman, G. Senn, G. Denifl, D. Muigg, J.D. Skalny, P. Lukac, A. Stamatovic, T.D. Märk, Czech. J. Phys. 48 (1998) 1135.
[26] G. Denifl, D. Muigg, I. Walker, P. Cicman, S. Matejcik, J.D. Skalny, A. Stamatovic, T.D. Märk, Czech. J. Phys. 49 (1999) 383.
[27] A.D. Bass, M. Lezius, P. Ayotte, L. Parenteau, P. Cloutier, L. Sanche, J. Phys. B 30 (1997) 1.
[28] M.N. Hedhili, R. Aria, Y. LeCoat, M. Tronc, Chem. Phys. Lett. 268 (1997) 21.
[29] E. Krishnakumar, S.K. Srivastava, Phys. Rev. A 41 (1990) 2445.
[30] Y. LeCoat, N.M. Hedhili, R. Aria, M. Tronc, O. Ingolfsson, E. Illenberger, Chem. Phys. Lett. 296 (1998) 208.
[31] P. Tegeder, F. Brüning, E. Illenberger, Chem. Phys. Lett. 310 (1999) 79.
[32] F. Brüning, P. Tegeder, J. Langer, E. Illenberger, Int. J. Mass Spectrom., submitted.
[33] J. Langer, S. Matt, M. Meinke, P. Tegeder, A. Stamatovic, E. Illenberger, J. Chem. Phys., in print (2000).
[34] S. Matejcik, G. Senn, P. Scheier, A. Kiendler, A. Stamatovic, T.D. Märk, J. Chem. Phys. 107 (1997) 8955.
[35] C.E. Klots, J. Chem. Phys. 46 (1967) 1197; Chem. Phys. Lett. 38 (1976) 61.
[36] D. Klar, M.W. Ruf, H. Hotop, Aust. J. Phys. 45 (1992) 263; Chem. Phys. Lett. 189 (1992) 448.
[37] NIST tables, http://webbook.nist.gov.
[38] A. Stamatovic, G.J. Schulz, J. Chem. Phys. 53 (1970) 2663.
[39] P.J. Chantry, Phys. Rev. 172 (1968) 125.
[40] K.P. Huber, G. Herzberg, Molecular Spectra and Molecular Structure IV, Van Nostrand, New York, 1979.
[41] D.M. Neumark, K.R. Lykke, T. Anderson, W.C. Lineberger, Phys. Rev. A 32 (1985) 1890.
[42] G. Hanel, T. Fiegele, A. Stamatovic, T.D. Märk, Z. Phys. Chem., 214 (2000) 1137.

[43] D.G. Hopper, A.C. Wahl, R.L.C. Wu, T.O. Tiernan, J. Chem. Phys. 65 (1978) 5474.
[44] W.E. Wentworth, E. Chen, R. Freeman, J. Chem. Phys. 55 (1971) 2075.
[45] S. Matejcik, P. Eichberger, B. Plunger, A. Kiendler, A. Stamatovic, T.D. Märk, Int. J. Mass Spectrom. Ion Processes 144 (1995) L13.
[46] C.E. Klots, Radiat. Phys. Chem. 20 (1985) 51.
[47] M. Foltin, V. Grill, T.D. Märk, Chem. Phys. Lett. 188 (1992) 427.
[48] O. Ingolffson, E. Illenberger, Int. J. Mass Spectrom. Ion Processes 149/150 (1995) 79.
[49] P.J. Chantry, J. Chem. Phys. 55 (1971) 1851.